THE SANTANA PROJECT

Alexander Geise[1], Arne F. Jacob[1], Karsten Kuhlmann[1], Holger Pawlak[1]
Roman Gieron[2], Patrice Siatchoua[2], Dirk Lohmann[2], Sybille Holzwarth[2], Oliver Litschke[2]
Marcos V. T. Heckler[3], Lukasz Greda[3], Achim Dreher[3]
Christian Hunscher[4]
[1]TU Hamburg-Harburg, Institut für Hochfrequenztechnik, 21071 Hamburg, Germany, Tel. +49 40428783019, jacob@tuhh.de
[2]IMST GmbH, 47475 Kamp-Lintfort, Germany, Tel. +49 2842981323, holzwarth@imst.de
[3]DLR, Institut für Kommunikation und Navigation, 82230 Wessling, Germany, Tel. +49 8153282314, achim.dreher@dlr.de
[4]Astrium GmbH, 81663 München, Tel. +49 8960720530, Christian.hunscher@astrium.eads.net

Abstract—**This paper deals with a modular Rx- and Tx-antenna terminal featuring digital beamforming (DBF) at Ka-band frequencies. Background and vision of the project SANTANA II and recent realizations are described. Different system components are outlined covering digital baseband, RF- and IF-level as well as software aspects. An outlook on mobile field tests, which will be reported at the conference, concludes this contribution.**

1. INTRODUCTION

Smart antennas employing Digital Beam Forming (DBF) at Ka-band frequencies will be key elements for the next generation of broadband satellite communication systems. This frequency band offers high bandwidth and corresponding data rate capability, whereas Digital Beam Forming provides ultimate system flexibility.

In order to optimize the performance the terminal antenna is divided into two separate arrays, one for the Receive (Rx, 20 GHz) and the other for the Transmit (Tx, 30 GHz) frequency band. With respect to the realization of large arrays the two antennas are composed of 4×4 array modules as basic building blocks.

Within the framework of Phase 1 (2001-2003) and Phase 2 (2003 - 2007) of the project Smart Antenna Terminal (SANTANA), funded by the German Space Agency (DLR) on behalf of the German Ministry of Economics and Technology (BMWi), key elements of advanced satellite communication terminals (e.g. for later implementation on aircrafts) at Ka-Band frequencies have been investigated. The goal was to develop and realize a 64 element DBF array allowing for the data exchange with moving platforms. Meanwhile, Phase 3 has started with, as main targets, further verification of the terminal itself within a moving environment, the adaptation of the current technology towards the realization of large arrays and the industrialization of several building blocks.

The Project Phase 2 was performed by a team consisting of the Institut für Hochfrequenztechnik at the Technische Universität Hamburg-Harburg, IMST GmbH at Kamp-Lintfort, DLR at Oberpfaffenhofen (Institut für Kommunikation und Navigation) and Astrium GmbH, Ottobrunn. In parallel the industrial feasibility of the concept was investigated by LEWICKI microelectronic GmbH, Oberdischingen.

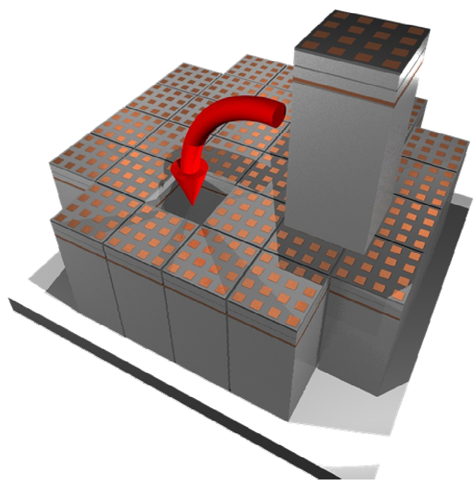

FIG. 1. Modular architecture of the DBF terminal antenna.

2. SYSTEM OVERVIEW

This section describes the overall system design, which is essentially the same for the receiver and the transmitter terminal antenna. A modular concept as depicted in FIG. 1 is used for construction of the terminal antennas.

One module consists of 16 patch antennas and the corresponding electronics for RF and IF circuitry. By adapting the number of modules it is possible to realize antenna arrays of any size according to the desired application. Further, individual modules are easily replaced or repaired. In the Santana II project an array consisting of four modules (64 patch antennas) has been realized. For communications between GEO-satellites and aircrafts typically more than 100 modules are needed.

The signals at 20 GHz for receive and 30 GHz for transmit determine the dimensions of the modules since the spacing of the patch antennas has to be half the wavelength. Therefore, the resulting areas of the modules are 30 x 30 mm^2 and 20 x 20 mm^2 for receiver and transmitter, respectively. This small size leads to a high integration density for the active and passive components.

The base plate, on which the modules are mounted, provides central functions like clock and LO generation, power supply, and cooling. FIG. 2 shows a photography of the Rx terminal which is subdivided into the highlighted parts: antenna and front-end, IF-boards, channel boards, power board, and mainboard.

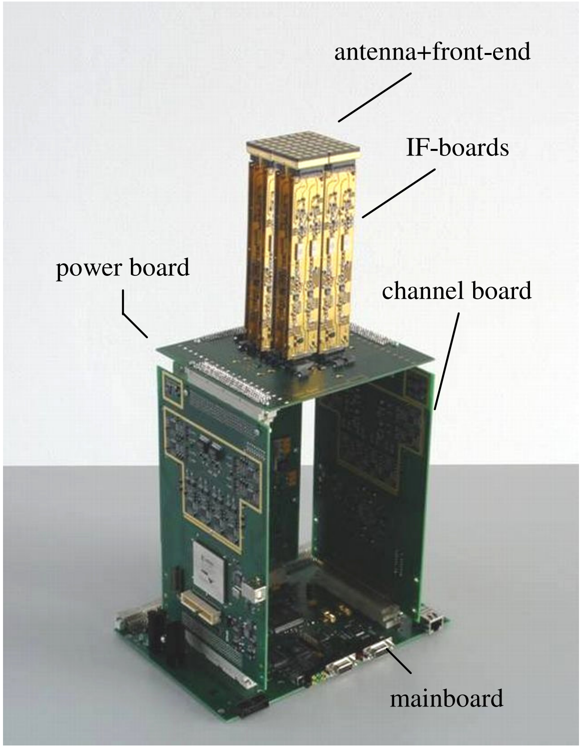

FIG. 2. Rx DBF terminal antenna.

3. RX- AND TX-ANTENNA

3.1 Rx-Antenna

The receiver antenna array operates at 19.7 – 20.2 GHz with left-handed circular polarization (LHCP). It is composed of square patches with truncated corners. The single element is sketched in FIG. 3. In receiving mode, the energy is coupled from the patch to a stripline through an aperture. Then, by means of the HF-via, the stripline is connected to a coplanar waveguide (CPW), which transmits the signal to the MMIC. The other vias shown in FIG. 3 interconnect all ground planes in the layered structure.

Two prototypes of single elements have been tested. In FIG. 4, a comparison between the simulated and measured return loss is presented. The deviations between the simulated and measured curves are due to manufacturing tolerance.

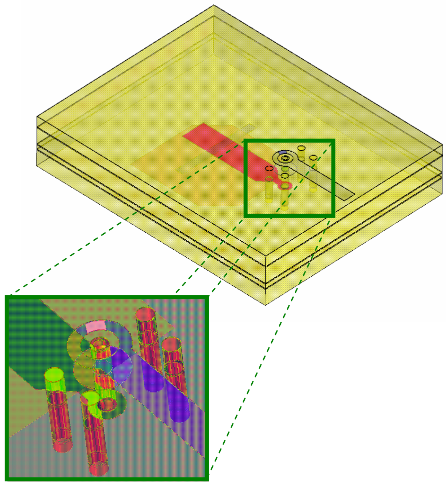

FIG. 3. Single element of the receiver antenna array. The transition between the stripline (red) and the CPW (gray) is shown in detail.

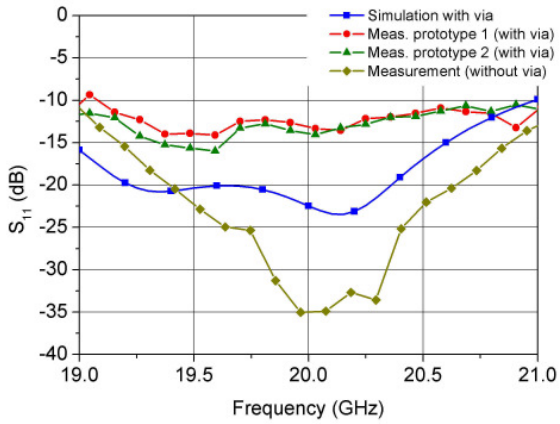

FIG. 4. Comparison between simulated and measured return loss of two different prototypes.

(a) (b)

FIG. 5. One module of the receiver antenna array: (a) top and (b) bottom view.

As mentioned above the receiver antenna array has been designed using a modular concept, where each module is composed of 16 patches arranged in a 4×4 configuration. The orientation of the single elements in the array is shown in FIG. 5, where the classical sequential rotation has been modified to improve the performance mainly in terms of polarization purity.

3.2 Tx-Antenna

The Tx-Antenna is a circularly polarized 8×8 element array consisting of four 4×4 basic building blocks with integrated calibration network. FIG. 6 shows the rather complex architecture of a single antenna element, consisting of eleven layers of LTCC substrates [1].

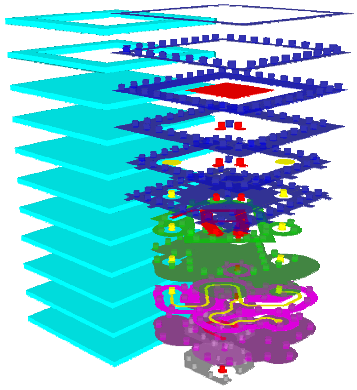

FIG. 6. Eleven layer structure of one antenna element.

Four different functional blocks can be identified within this buildup: the antenna block is depicted in blue (cavity-buried patches assuring good decoupling), the green block marks the hybrid ring coupler (for excitation of circular polarization), the purple parts define a part of the calibration network, and the RF-to-antenna interface is shown in grey. The transmit signal path is marked in red going from the bottom of the structure to the patch at the top, while the yellow path shows the calibration signal path.

The EM-simulation model of one 4×4 array building block and the complete 8×8 array, consisting of four building blocks, is shown in FIG. 7.

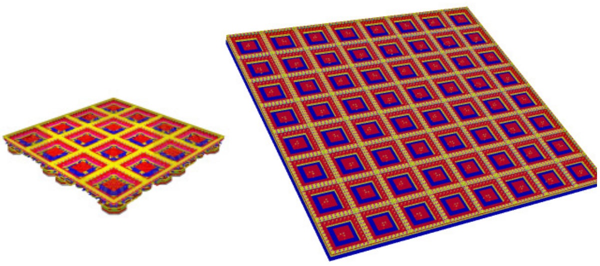

FIG. 7. EM-Simulation model of the 4×4 array building block (left) and the complete 8×8 array (right).

Reflection coefficients and polarisation behaviour of the antenna elements have been measured [2]. A good agreement with the computed results can be stated. In addition, a good reproducibility of the manufacturing process was found. The far field characteristics of the complete 8x8 array, steered to different angles, are also in excellent agreement with the computed results.

4. ANALOG CIRCUITRY AND ARCHITECTURE

Each RF chipset includes an amplifier, image reject filter, and mixer, which consist of Monolithic Microwave Integrated Circuits (MMICs). The MMICs are mounted on the front-end multilayer and are embedded in cavities at the bottom side of the antenna multilayer. The supply network, local oscillator divider network, and IF outputs are integrated into the front-end. The antenna is mounted on top using anisotropically conductive adhesives for reliable RF interconnections [3], whereas a cooling plate is bonded on its bottom side. Efficient water cooling is applied to remove the heat arising from the embedded amplifiers and is packaged between the manifold and front-end modules. FIG. 8 shows a schematic representation of the Rx- and Tx-module architecture.

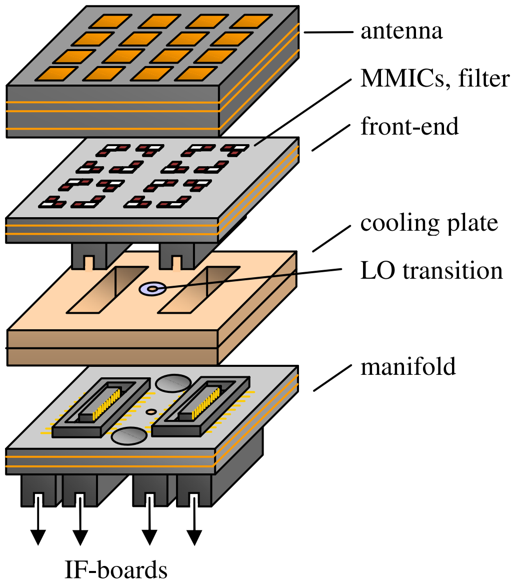

FIG. 8. Module architecture.

For both Rx- and Tx-circuits, a harmonic frequency conversion approach has been used to facilitate filtering and amplification at IF frequencies, where a wide variety of commercial components is available. The subharmonically pumped mixers at Ka-band simplify the design due to the lower LO frequencies and reduce distribution losses. The equivalent circuit diagrams of the chipsets for Rx and Tx are depicted in FIG. 9.

The Rx-circuit is designed for low noise FIG. and high amplification. The gain is controllable at two IF frequencies to compensate for channel variations and to increase the dynamic range at the IF output. An automatic gain control adjusts the output power according to the received signal strength. This ensures optimal drive of the A/D-converter. A total gain of more than 100 dB is provided. Channels of 20 MHz bandwidth can be selected from a RF bandwidth of 500 MHz.

Instead of noise figure and gain, the Tx circuitry is optimized for high RF output power. Medium power amplifiers (MPA) yield the best compromise between power consumption, thermal management, physical dimension and output power. Channel gain variations can be compensated by variable gain IF amplifiers. At 30 GHz an output power of 6-8 dBm can be achieved.

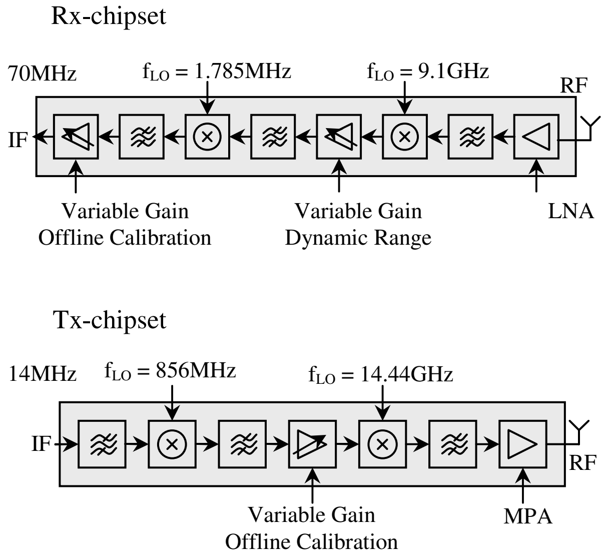

FIG. 9. Equivalent circuit diagrams for Rx and Tx.

The transmit antenna array can be calibrated by two independent calibration systems. The first one extracts calibration information for each patch by evaluating the field in the vicinity of the array by means of small calibration antennas at 30 GHz [4]. The second one uses a calibration network implemented in the LTCC multilayer (see above). The output signal of the calibration networks are downconverted to IF on the frontend. Both calibration systems are connected to external calibration receivers for further signal processing like low-noise amplification and final downconversion to baseband. The amplitude and phase of the baseband signal is estimated from a number of samples and the calibration is performed by the algorithms for each calibration system.

5. ANTENNA CONTROL AND DATA PROCESSING

5.1 Digital Signal Processing Hardware

The digital signal processing hardware of the Tx- and Rx-system, respectively, consists of four different functional blocks: the Rx channel board depicted in FIG. 10 provides the signal down-conversion for each channel (one for each antenna element), the beamsteering, and signal summation. Respectively, the Tx channel board, depicted in FIG. 11, provides the beam steering and up-conversion of the transmitted signals.

The data is transmitted or received by the baseband main boards depicted in FIG. 12. Alternatively, the signal can also be processed by an external satellite modem. For the transmitter, data rates up to 400kbps can be handled, while the receiver can cope with data rates up to 20Mbps.

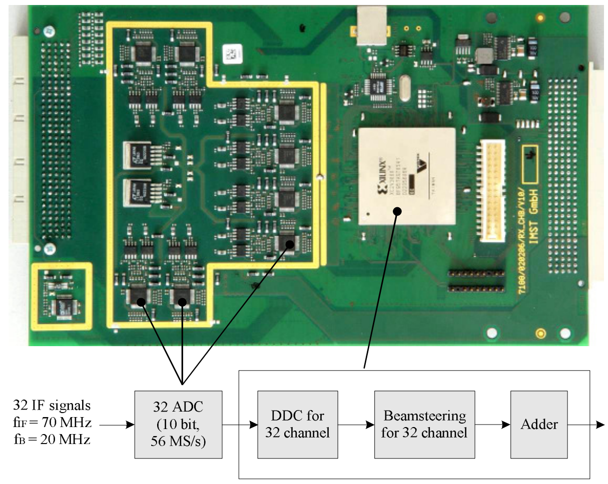

FIG. 10. Rx Channel Board.

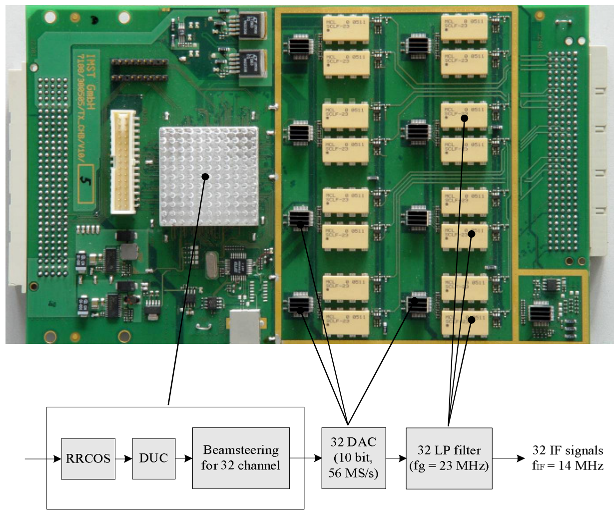

FIG. 11. Tx Channel Board.

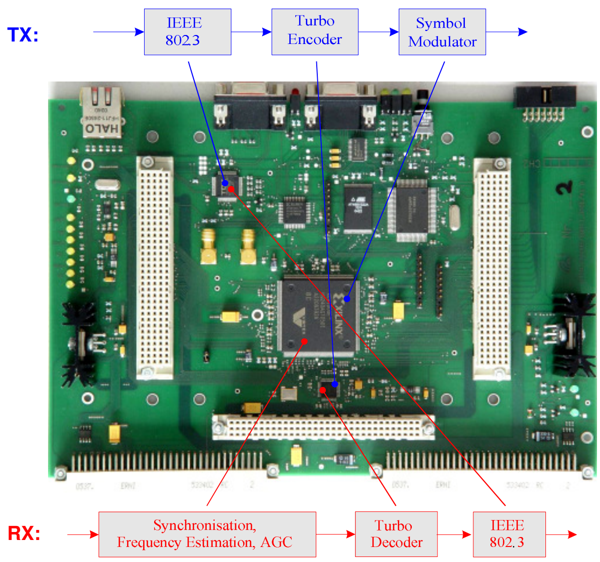

FIG. 12. Base Band Main Board.

Tx and Rx Power Boards (not depicted) provide the power supply for the RF and IF Boards, while Tx and Rx distribution boards (not depicted) ensure the distribution of the signals to/from the IF Boards.

5.2 Beamforming Algorithm

The beamforming algorithm provides dedicated amplitude and phase for each antenna channel of the Rx or Tx antenna for a given antenna pointing direction and a given performance (e.g. side lobe level).
The antenna pointing direction could be provided by an external navigation system (e.g. GPS system). Alternatively the SANTANA system can generate this information self-contained on the basis of "direction-of-arrival" (DOA) estimation and tracking algorithms.

5.3 DOA algorithm

The DOA algorithm uses the incoming signals of all Rx antenna channels to calculate apriori unknown direction of the incoming wave. It can also be used to track moving communication targets. However, if the target is moving continuously without jerky leaps or erratic movements, special tracking algorithms can be applied to follow the target requiring low computational effort once the direction of the incoming wave has been calculated using the DOA algorithm.

5.4 Tracking Algorithm

The tracking algorithm compares the received signal from the most recent antenna pointing direction with those from adjacent pointing directions. If the communication target moves, one of the adjacent pointing directions will become the new pointing direction. In comparison to the DOA algorithm, the tracking algorithm needs less computational time. On the other hand, the algorithm is dependant on a correct initial pointing value. Therefore, the SANTANA system combines DOA and tracking algorithms. The initial value is computed by the DOA algorithm, the tracking algorithm is then applied for tracking the moving communication target. If somehow the tracked signal is lost (e.g. due to disturbances), the DOA algorithm will compute a new initial value.

5.5 Graphical User Interface

For system calibration and basic functionality tests, both Rx and Tx antennas can be controlled manually using graphical user interfaces, which allow to turn individual antenna elements on or off, apply phase offsets or calibration values or point the antenna to any direction.
During data communication tests, however, the system is in an automatic mode, while important system parameters (e.g. current DOA position, pointing direction or signal power level) can be monitored.

6. SYSTEM TEST AND DEMONSTRATION

6.1 Calibration and Laboratory Tests

Prior to the final data communication test, extensive laboratory tests were needed to verify the system functionality. First, the system was calibrated and the far field characteristics of the Rx- and Tx-antenna were measured for different steering angles.

Subsequently, basic system functionality tests had to be performed. For example, the DOA algorithm and the tracking capabilities of the Rx system had to be tested using a measurement setup with a mobile signal generator as depicted in FIG. 13.

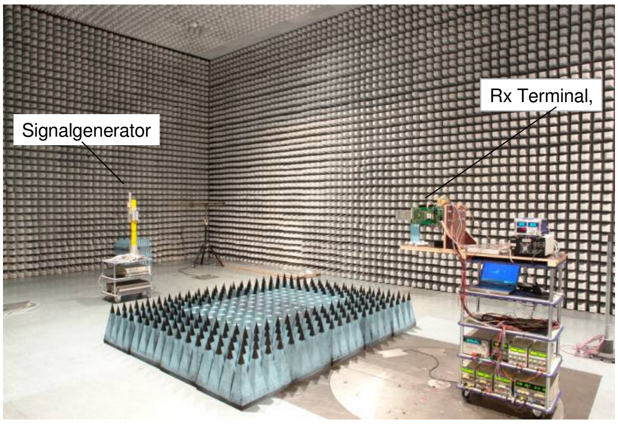

FIG. 13. Test of the DOA algorithm and the tracking capabilities of the Rx system.

6.2 Data Communication with Demonstration Vehicule

The data communication between the SANTANA system and a moving platform has been successfully demonstrated on the premises of IMST. FIG. 14 shows the location of the SANTANA system at the window of the second floor of the IMST building and the demonstration vehicle in the outdoor test range at a distance of about 80 m. While the test vehicle was moving, undisturbed data communication (e.g. video conferencing) of the SANTANA system and the demonstration vehicle was possible.

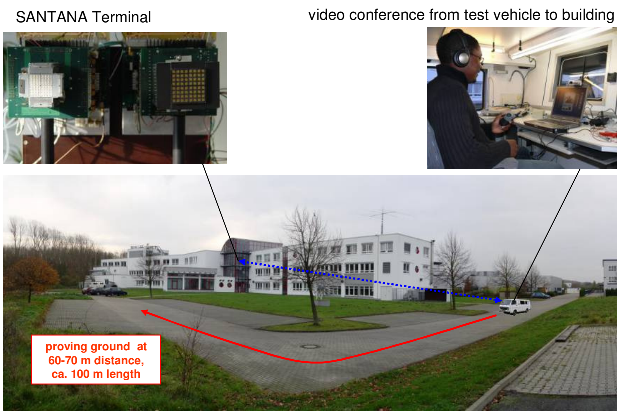

FIG. 14. Communication with moving demonstration vehicle.

6.3 Airborne Field Tests

FIG. 15 illustrates a basic test scenario of the airborne field test which concluded project phase 2. A Ka-band transponder system (beacon) was mounted on an experimental aircraft of TU Braunschweig, Germany. The antennas of the beacon are open ended waveguides featuring left-handed circular polarization and a 3 dB beamwidth of 70° to illuminate a large spot on the ground. The aircraft flew circles around the terminal antennas and a mechanically steered reference system (not shown). The key parameters of the scenario are the circle diameter D, the height h and the aircraft velocity v. The advantage of this scenario is a constant look angle θ and a constant angular velocity ω. This scenario was primarily used to establish the link and record basic system parameters (received power level, signal-to-noise ratio, required channel gain, required channel coding to realize specified BER, etc.). This was done for both the terminal antennas and the reference system. The aim was to calculate a realistic link budget for larger terminal antennas from the data taken during the test scenario. Afterwards the ability of the terminal to acquire and point at the aircraft was tested. The aircraft position estimated by the direction-of-arrival algorithm (DOA) was compared to the actual position recorded by the aircraft's inertial navigation system. After successful completion of the outlined measurements the tracking ability of the terminal was tested by more dynamic scenarios including direct overflights in various heights. By this way, the tracking performance of the terminal could be tested for different angular velocities.

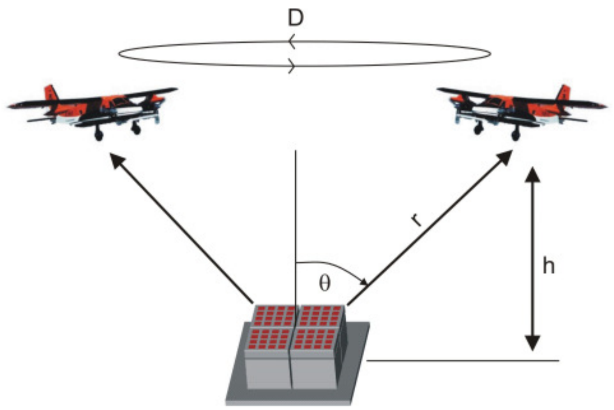

FIG. 15. Basic scenario of the airborne field test.

7. CONCLUSION

In this paper the background and the goals of the SANTANA II project have been presented. With the experience gained from the project phase I, the novel elements of the terminal architecture could be realized and measured successfully. An 8x8 technology demonstrator both for the receive and transmit function has been constructed and tested in different environments (laboratory, anechoic chamber, ground and airborne field tests). Results will be reported at the conference.

The modular architecture of the DBF terminal antenna is the basis for larger arrays able to comply with the distance and beam width requirements of future applications. The underlying technological issues are investigated in the current project phase 3 (SANTANA III).

ACKNOWLEDGMENT

The authors wish to acknowledge the funding of this work by the German Aerospace Center (DLR) on behalf of the German Federal Ministry of Economics and Technology (BMWi) under research contracts 50YB0304 and 50YB0311.

REFERENCES

[1] O.Litschke, W.Simon, S.Holzwarth; "A 30 GHz highly integrated LTCC antenna element for digital beam forming arrays", Antennas and Propagation Symposium, pp. 297-300, vol. 3B, Washington, July 2005.

[2] S.Holzwarth, O.Litschke "8x8 element digital beam forming antenna array for Ka-Band", 1st European Conference on Antennas and Propagation, Nice, November 2006.

[3] L.C. Stange, A. Geise, A.F. Jacob, "Highly Integrated 4x4 active array transmitter frontend for digital beamforming at 30 GHz", 34th European Microwave Conference, pp.295–298, Paris, Oct. 2005.

[4] H. Pawlak, A. Charaspreedalarp, A. F. Jacob, "Experimental Investigation of an External Calibration Scheme for 30 GHz Circularly Polarized DBF Transmit Antenna Arrays", Proceedings 36th European Microwave Conference, pp. 764–767, Manchester, September 2006.